Insights into Mercury's mantle composition from thermo-chemical evolution models

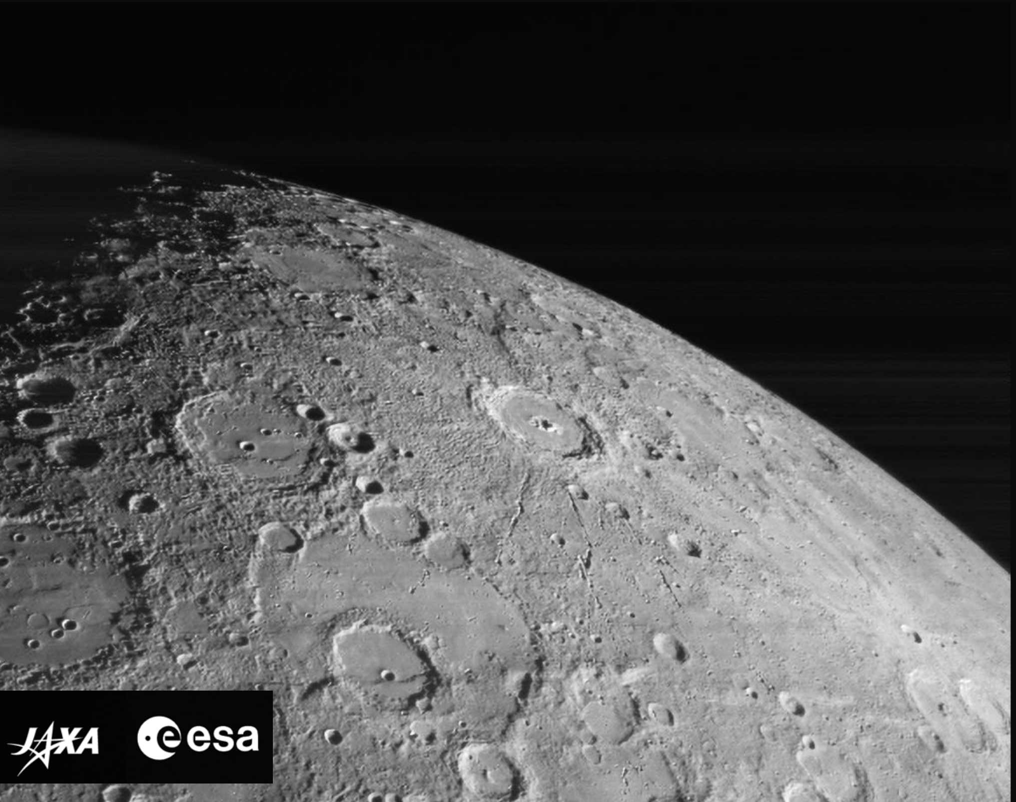

M. Lécaille, N. Tosi, A. Rivoldini, P. Baumeister,
O. Namur, B. Charlier

LIÈGE université
fnrs LA LIBERTÉ DE CHERCHER
DLR
Royal Observatory of Belgium
FREIE UNIVERSITÄT BERLIN
KU LEUVEN

How the choice of constraints impacts thermal evolution models of Mercury

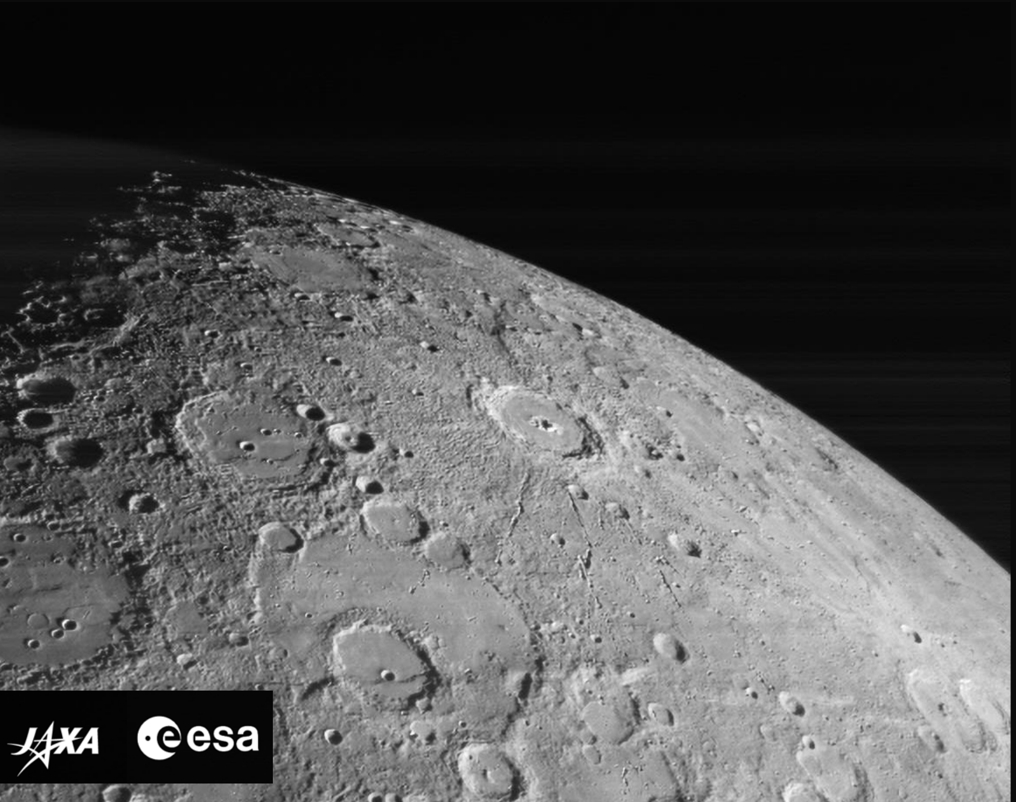

M. Lécaille, N. Tosi, A. Rivoldini, P. Baumeister, O. Namur, B. Charlier

Observations are difficult to reconcile in a single thermal evolution model

- Radial contraction — e.g. Di Achille et al., 2012, Byrne et al., 2014, Crane and Klimczak, 2017, Watters, 2021, Broquet and Andrews-Hanna, 2026
- Volcanic activity — e.g. Padovan et al., 2015, Byrne et al., 2016, Sori, 2018
- Dynamo — e.g. Johnson et al., 2015

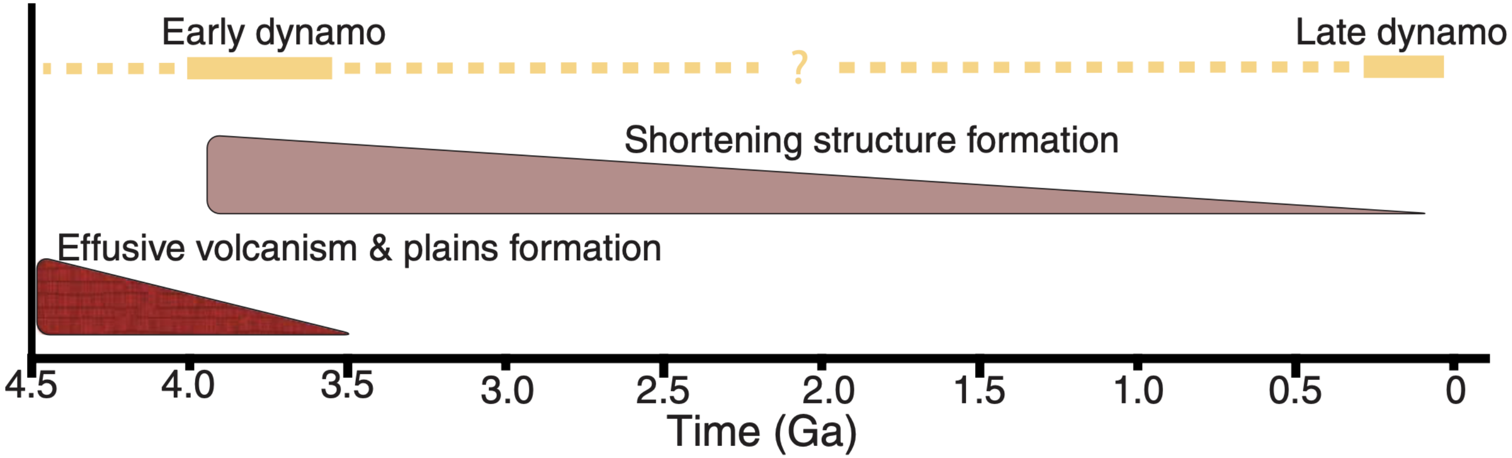

Peterson et al., 2021

We aim at refining Mercury's thermal evolution model

1. By running a set of MC simulations exploring a large parameter space
   (e.g. Grott et al. 2011, Tosi et al. 2013, Davies et al. 2024, Knibbe et al. 2025)

2. A-posteriori filter the results by selecting constraints individually

We aim at refining Mercury's thermal evolution model

1. By running a set of MC simulations exploring a large parameter space
   (e.g. Grott et al. 2011, Tosi et al. 2013, Davies et al. 2024, Knibbe et al. 2025)

2. A-posteriori filter the results by selecting constraints individually

3. Characterize successful models that satisfy all constraints

We aim at refining Mercury's thermal evolution model

1. By running a set of MC simulations exploring a large parameter space
   (e.g. Grott et al. 2011, Tosi et al. 2013, Davies et al. 2024, Knibbe et al. 2025)

2. A-posteriori filter the results by selecting constraints individually

3. Characterize successful models that satisfy all constraints

Very different thermal evolution models are needed to satisfy the different constraints
→ Only a few models can satisfy all constraints at once.

Constraints we considered:

0 Myr

500 Myr

1 Gyr

Today

Net contraction regime — Crane and Klimczak, 2017, Broquet and Andrews-Hanna, 2026

Ancient dynamo — Johnson et al., 2015 (E_j > 1 MW/K, Davies et al. 2024)

> 50% radial contraction — Crane and Klimczak, 2017, Broquet and Andrews-Hanna, 2026

> 90% crust produced — Byrne et al., 2016

Current dynamo — Johnson et al., 2015

Crust thickness between 15 and 60 km — Padovan et al., 2015, Sori, 2018

1-D parameterized mantle convection model

TEMPURA code Baumeister et al. (2023)

+ Melting:

Reduced CMAS mantle Namur et al. (2016)

+ Heat-producing elements:

EH chondrite Pirotte et al. (2023)

+ Density, heat capacity:

P-T-composition dependent
Mixture of forsterite, enstatite and diopside
Stixrude & Lithgow-Bertelloni (2005, 2024)

+ Thermal conductivity:

P-T-composition dependent
Mixture of forsterite Zhang et al. (2019),
enstatite Guo et al. (2024), and
diopside Wang et al. (2014).

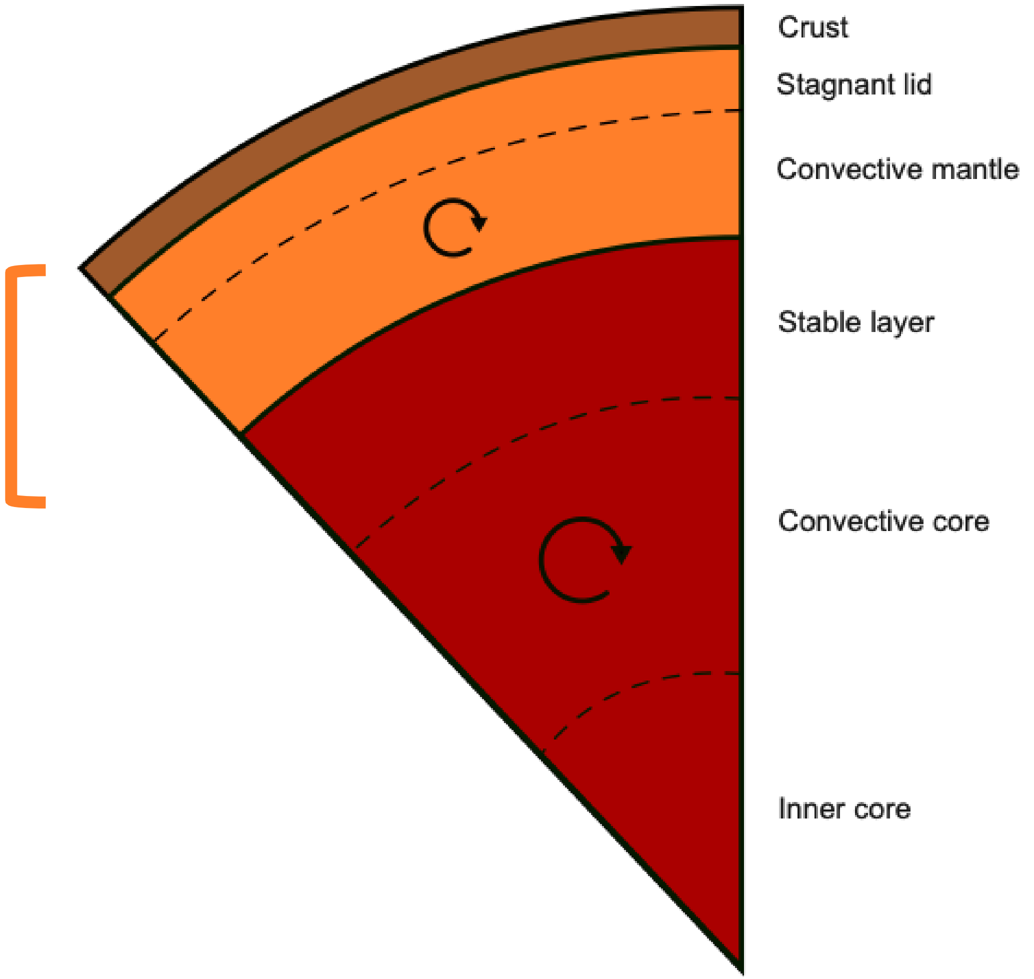

Core thermal evolution model

Thermal History code Greenwood et al. (2021)

+ self-consistent thermodynamic properties of Fe-Si alloys.

Equations of State:
Solid inner core: Edmund et al. (2019)
Liquid outer core: Terasaki et al. (2019)

Liquidus:
Fe: Dorogokupets et al. (2017)
Eutectic: Edmund et al. (2022)

$$\mathrm{T(p)}^{Fe-Si} = T^{Fe}(\mathrm{p}) - \left(T^{Fe}(\mathrm{p}) - T^{\mathrm{E}}(\mathrm{p})\right) \times \frac{x_{Si}}{x_{Si}^{E}}$$

Thermal conductivity:
Fe: Edmund et al. (in press)
$FeSi_{8.5wt.\%}$: Berrada et al. (2021)

$$\mathrm{k}^{-1} = \frac{1 - \mathrm{X_{Si}/X_{Si8.5}}}{\mathrm{k_{Fe}(p)}} + \frac{\mathrm{X_{Si}/X_{Si8.5}}}{\mathrm{k_{FeSi8.5}(p)}}$$

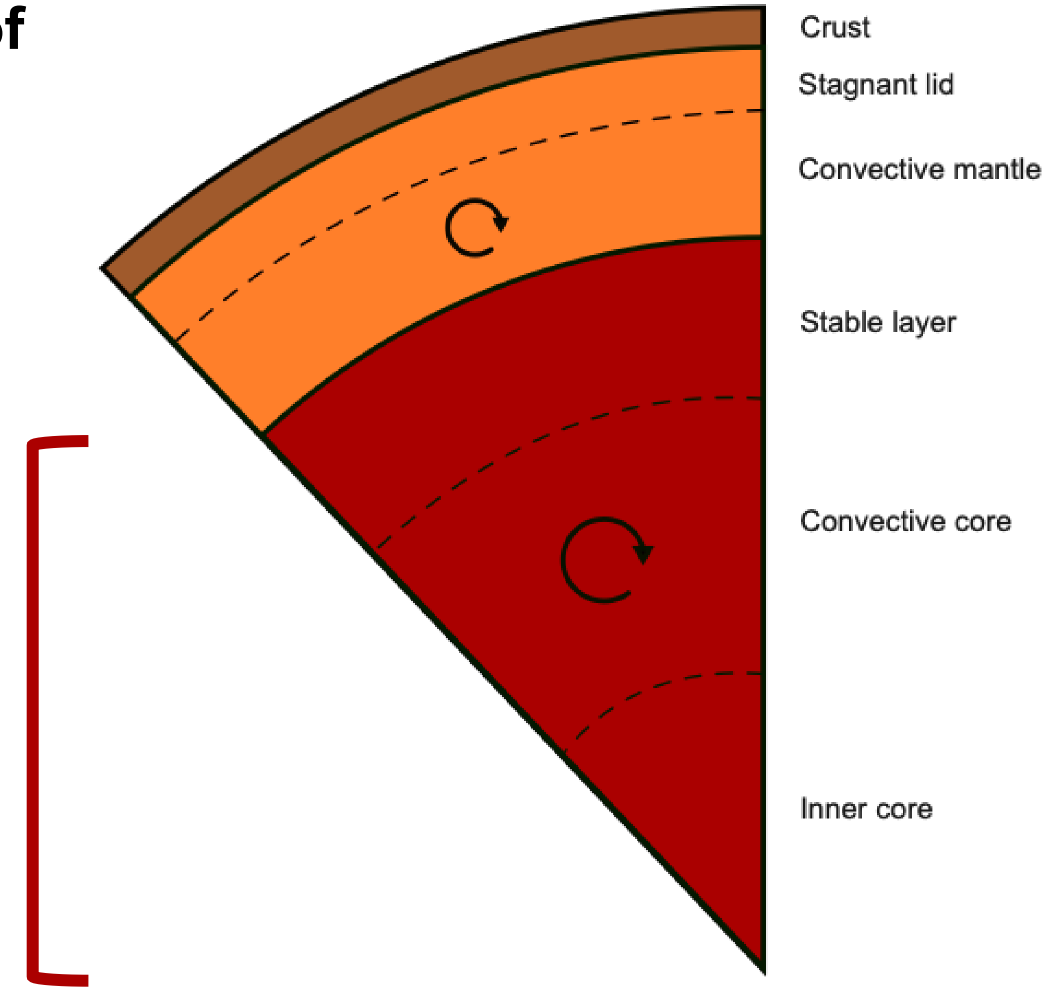

Model parameters:

50,000 simulations

• Mantle reference viscosity	$10^{19} – 10^{23}$ Pa s
• HPE crustal enrichment factor	2 – 20
• Enstatite-forsterite percentage (always 10% diopside)	0 – 90%
• Initial mantle temperature	1700 – 1800 K
• Initial CMB temperature	1850 – 2100 K
• Core radius	2000 – 2020 km

Model parameters:

50,000 simulations

- Mantle reference viscosity $10^{19} - 10^{23}$ Pa s
- HPE crustal enrichment factor 2 – 20
- Enstatite-forsterite percentage 0 – 90%
  (always 10% diopside)
- Initial mantle temperature 1700 – 1800 K
- Initial CMB temperature 1850 – 2100 K
- Core radius 2000 – 2020 km

Interior structure solved:

Core Si concentration adjusted to match bulk planet density

Model parameters:

Poorly constrained core properties:

- Core thermal conductivity: varied within experimental uncertainty

  At CMB: 25, 27, or 30 W m^{-1} K^{-1}

- Core melting entropy factor: increased by a factor of up to 1.5

  → Linked to latent heat released upon inner core growth

  At CMB: 7 – 10 J K^{-1} mol^{-1} ; 228 – 342 kJ kg^{-1}

Fraction of models satisfying single constraints:

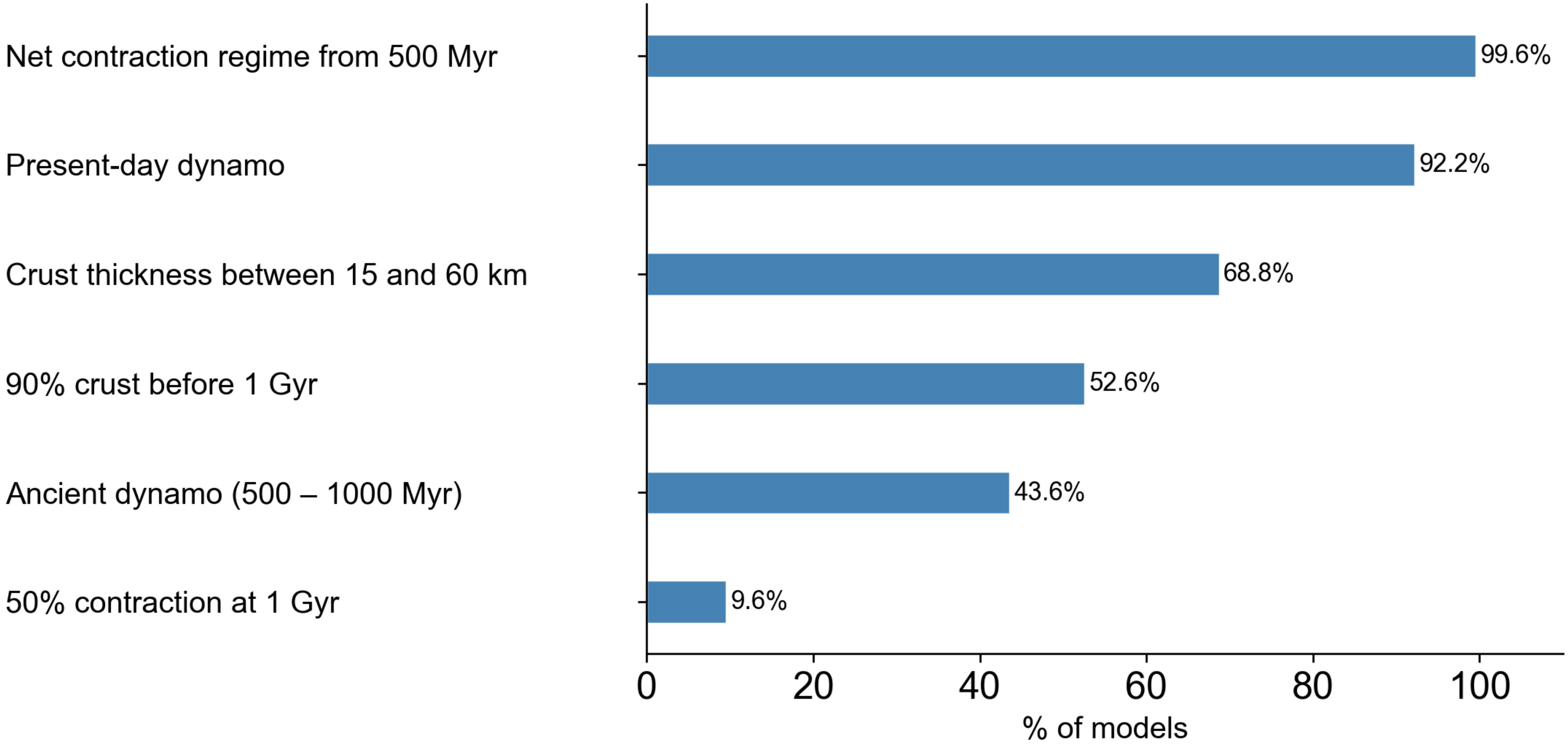

Fraction of models satisfying single constraints:

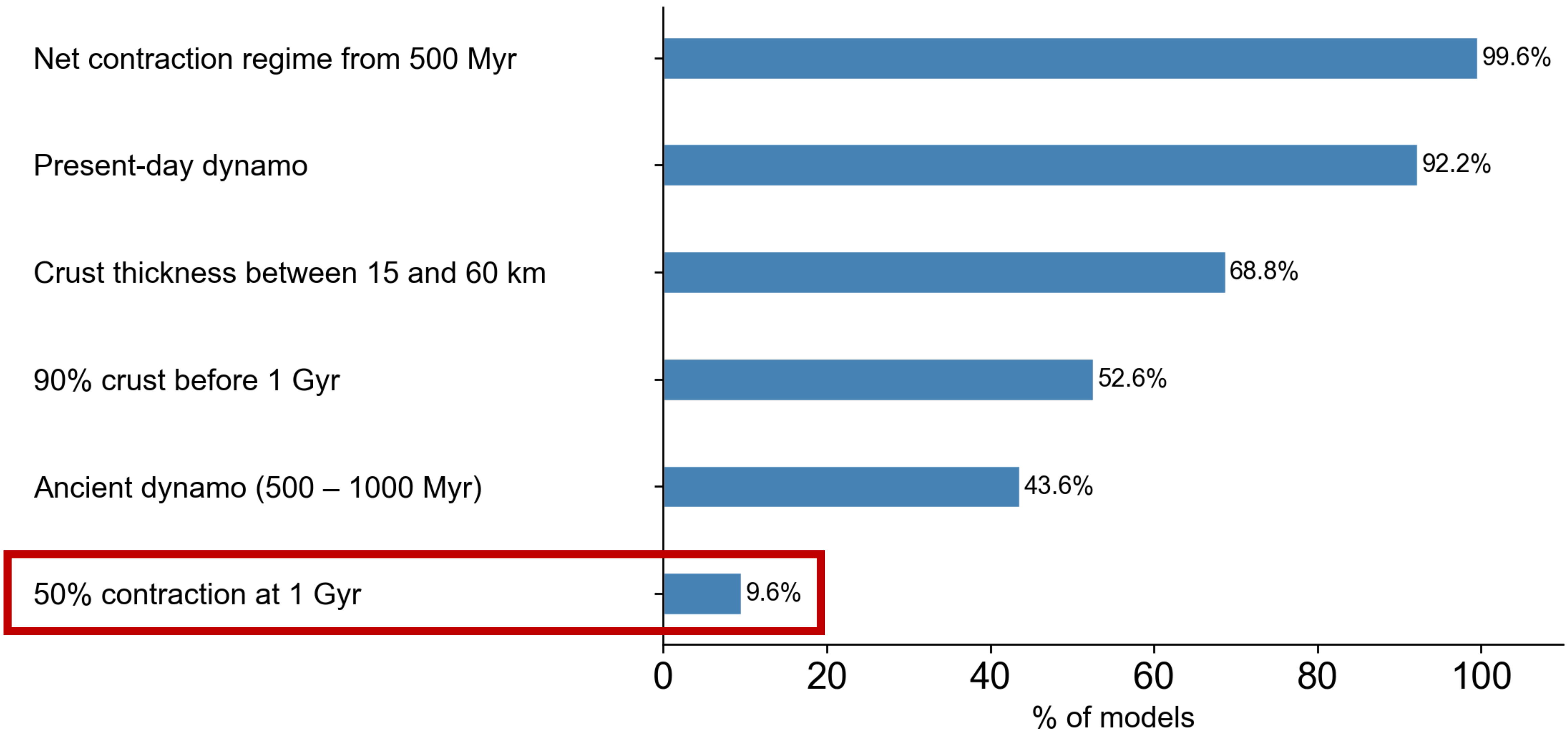

Models that reach 50% contraction by 1 Gyr are the most challenging

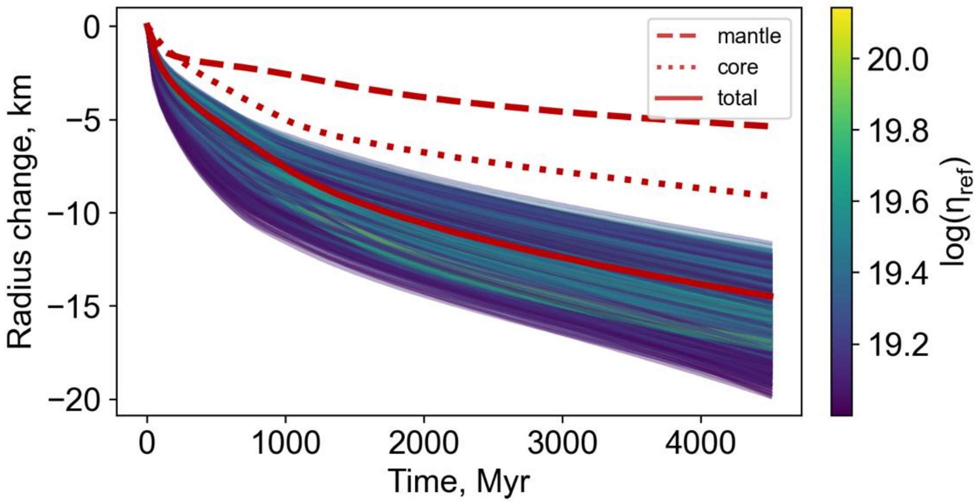

- Contract from the start.
- Core contribution to radial contraction more important than mantle contribution.

Models that reach 50% contraction by 1 Gyr are the most challenging

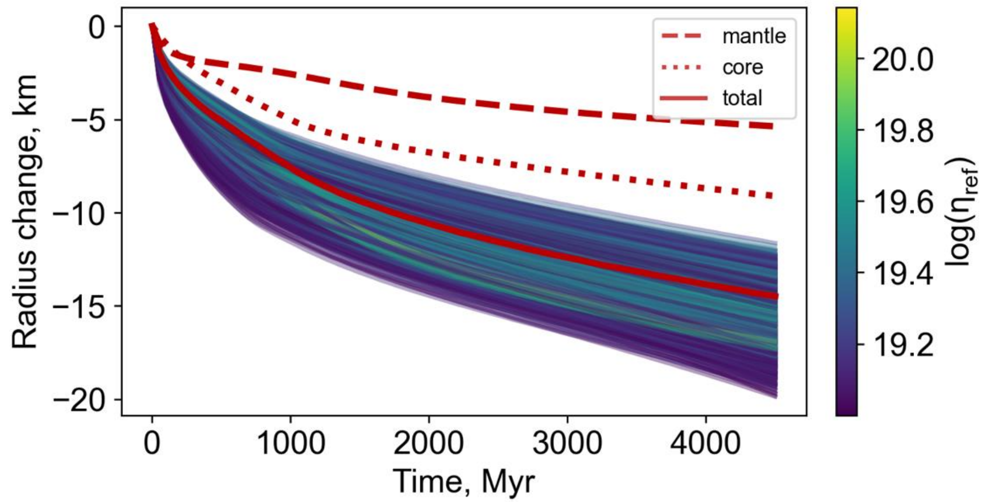

- Contract from the start.
- Core contribution to radial contraction more important than mantle contribution.
- Effective and fast mantle and core cooling.

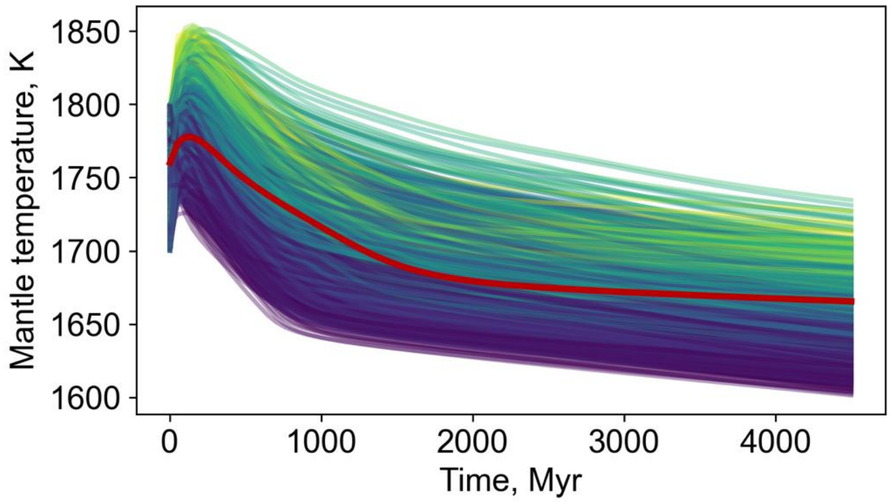

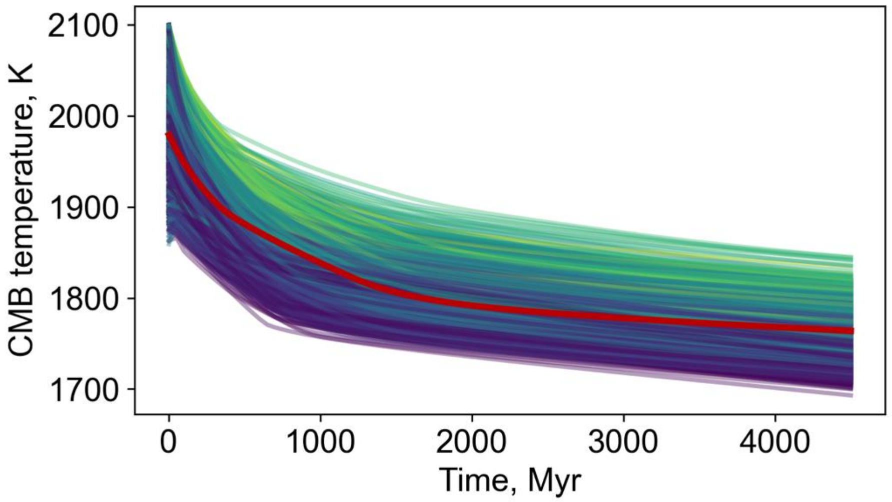

Models that reach 50% contraction by 1 Gyr are the most challenging

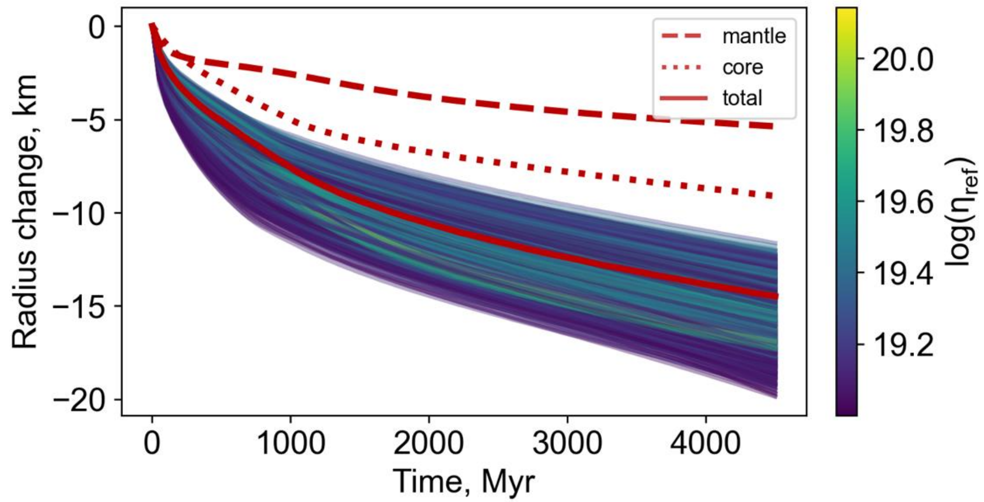

For lots of models:

- no dynamo action between 0.5 and 1 Gyr,
- or today,

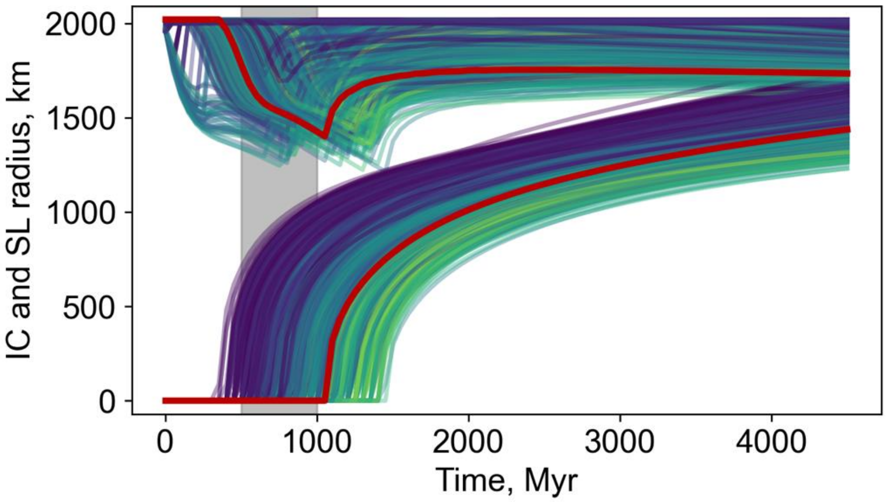

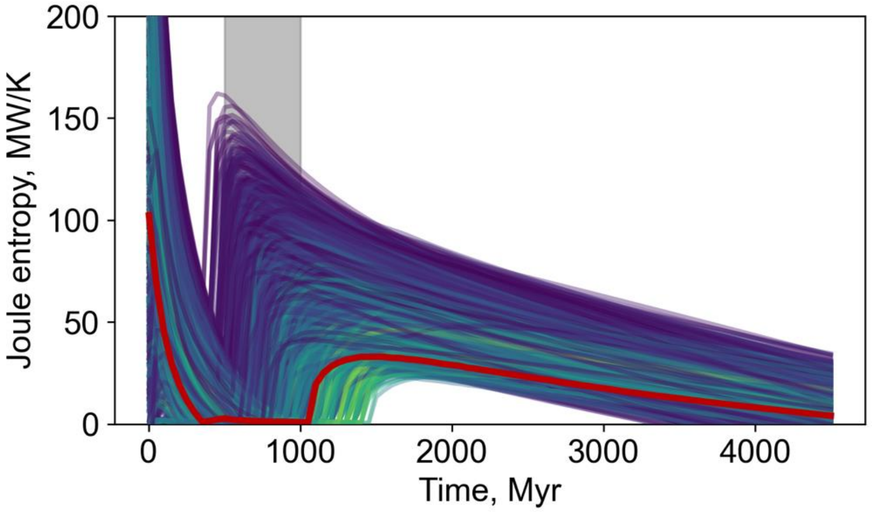

Models that reach 50% contraction by 1 Gyr are the most challenging

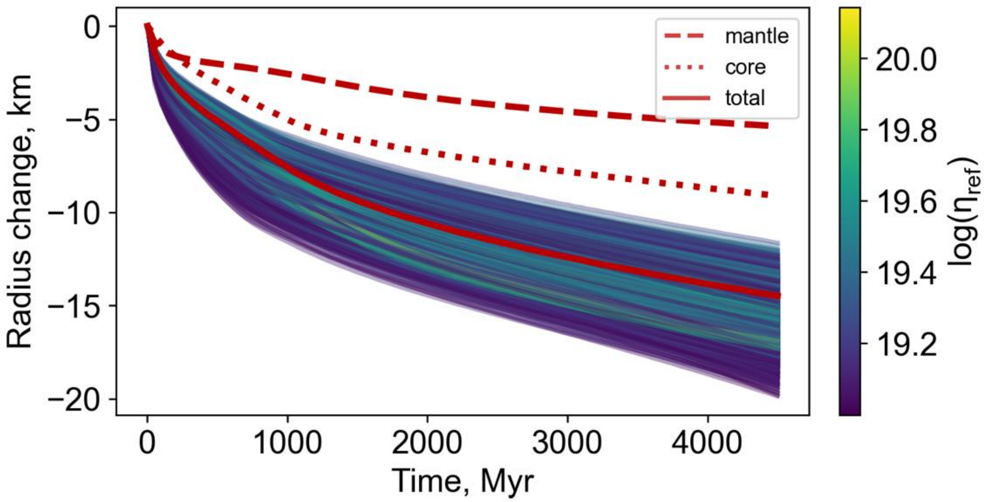

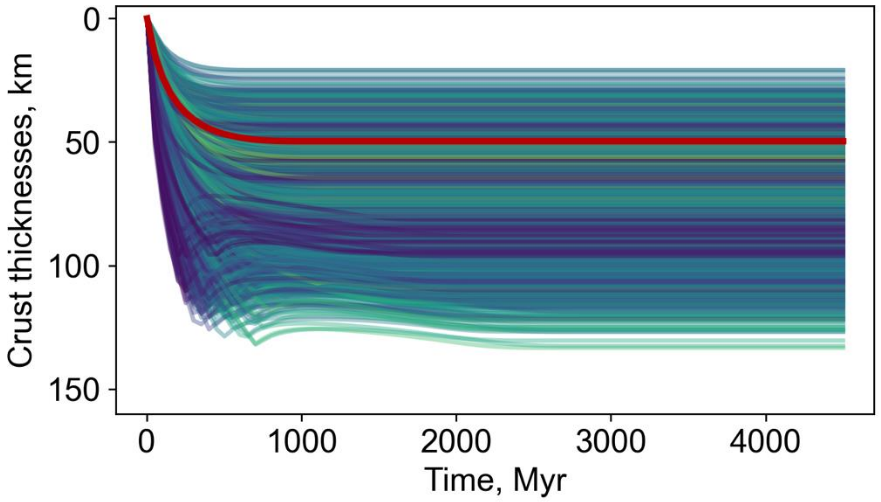

For lots of models:

- no dynamo action between 0.5 and 1 Gyr,
- or today,
- crust too thick

Distributions of mantle reference viscosity and initial CMB temperature for different constraints:

- To reach 50% contraction before 1 Gyr, models must have a low mantle reference viscosity and a high initial CMB temperature.

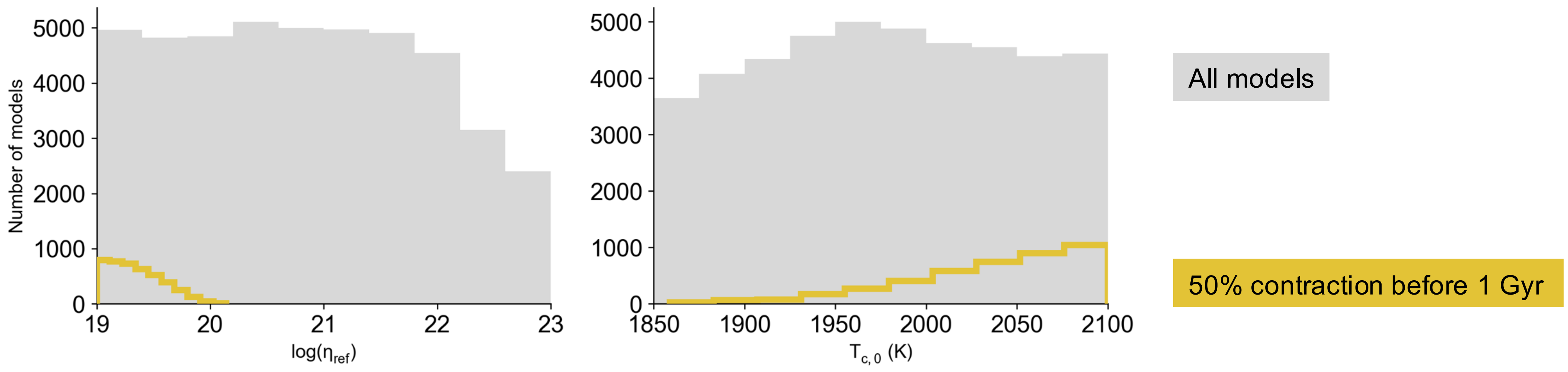

Distributions of mantle reference viscosity and initial CMB temperature for different constraints:

- To reach 50% contraction before 1 Gyr, models must have a low mantle reference viscosity and a high initial CMB temperature.

- Low mantle viscosities also helps model produce 90% of the crust before 1 Gyr and produce a dynamo between 0.5 and 1 Gyr.

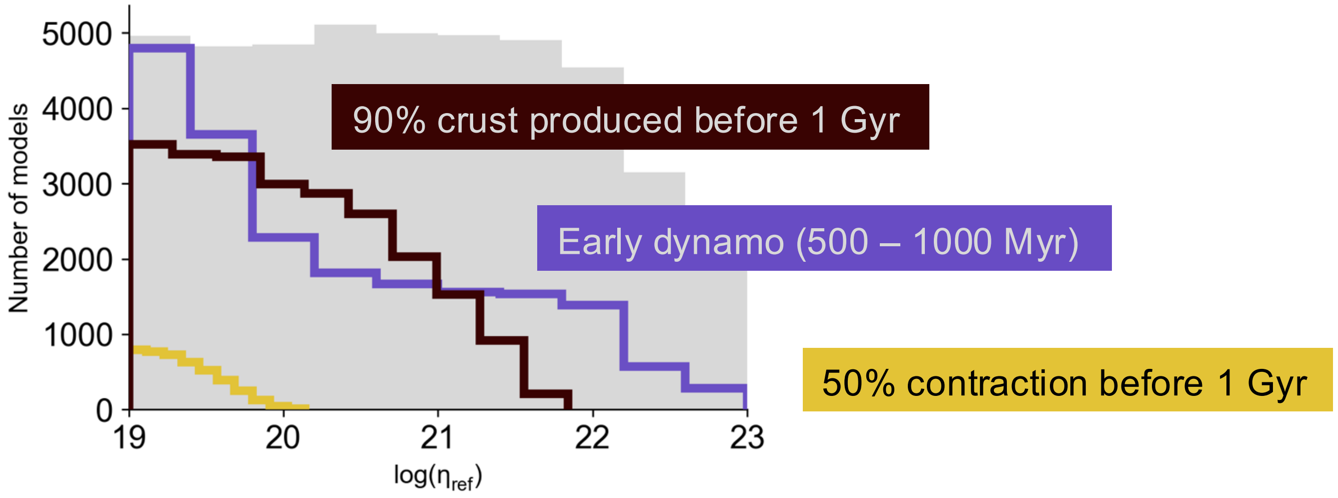

Distributions of mantle reference viscosity and initial CMB temperature for different constraints:

- To reach 50% contraction before 1 Gyr: low mantle reference viscosity, high initial CMB temperature.
- Low mantle viscosities also helps model produce 90% of the crust before 1 Gyr and produce a dynamo between 0.5 and 1 Gyr.
- Early dynamo generation is facilitated by lower initial CMB temperatures.

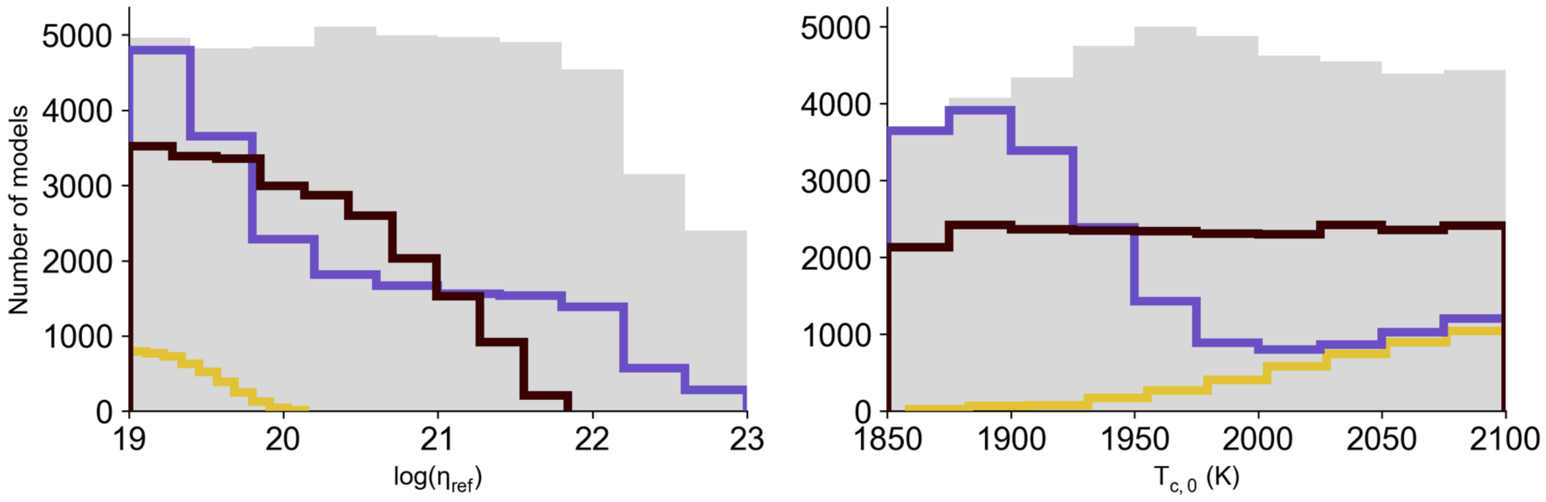

90% crust produced before 1 Gyr

Early dynamo (500 – 1000 Myr)

50% contraction before 1 Gyr

Distributions of mantle reference viscosity and initial CMB temperature for different constraints:

- Other constraints easier to satisfy with a larger reference viscosity:

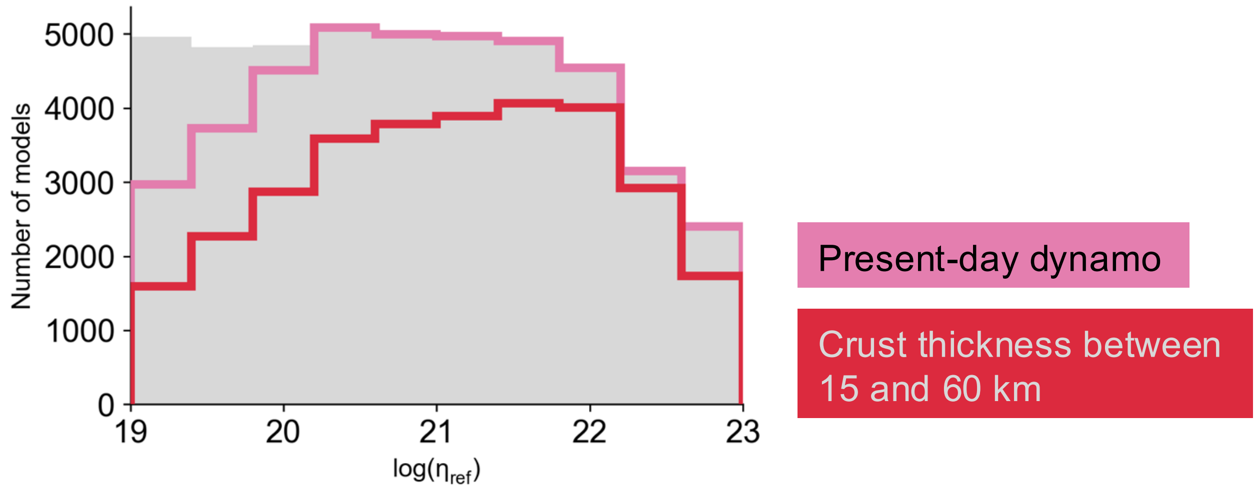

Can some models satisfy the following constraints combined?

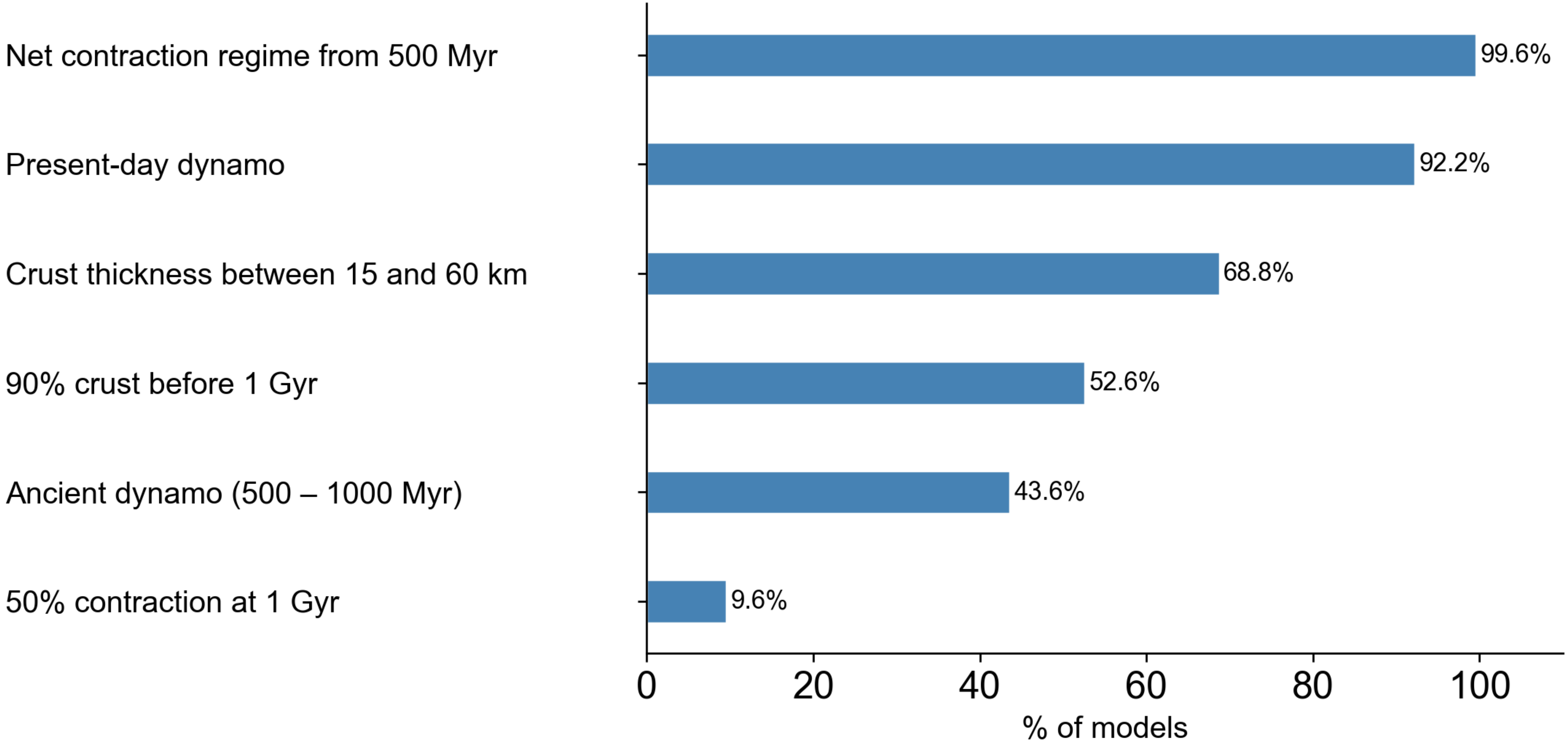

338 models (0.8%) satisfy all constraints

Crust thickness
Present-day and past dynamo
Early contraction regime
90% crust formed before 1 Gyr
50% contraction before 1 Gyr

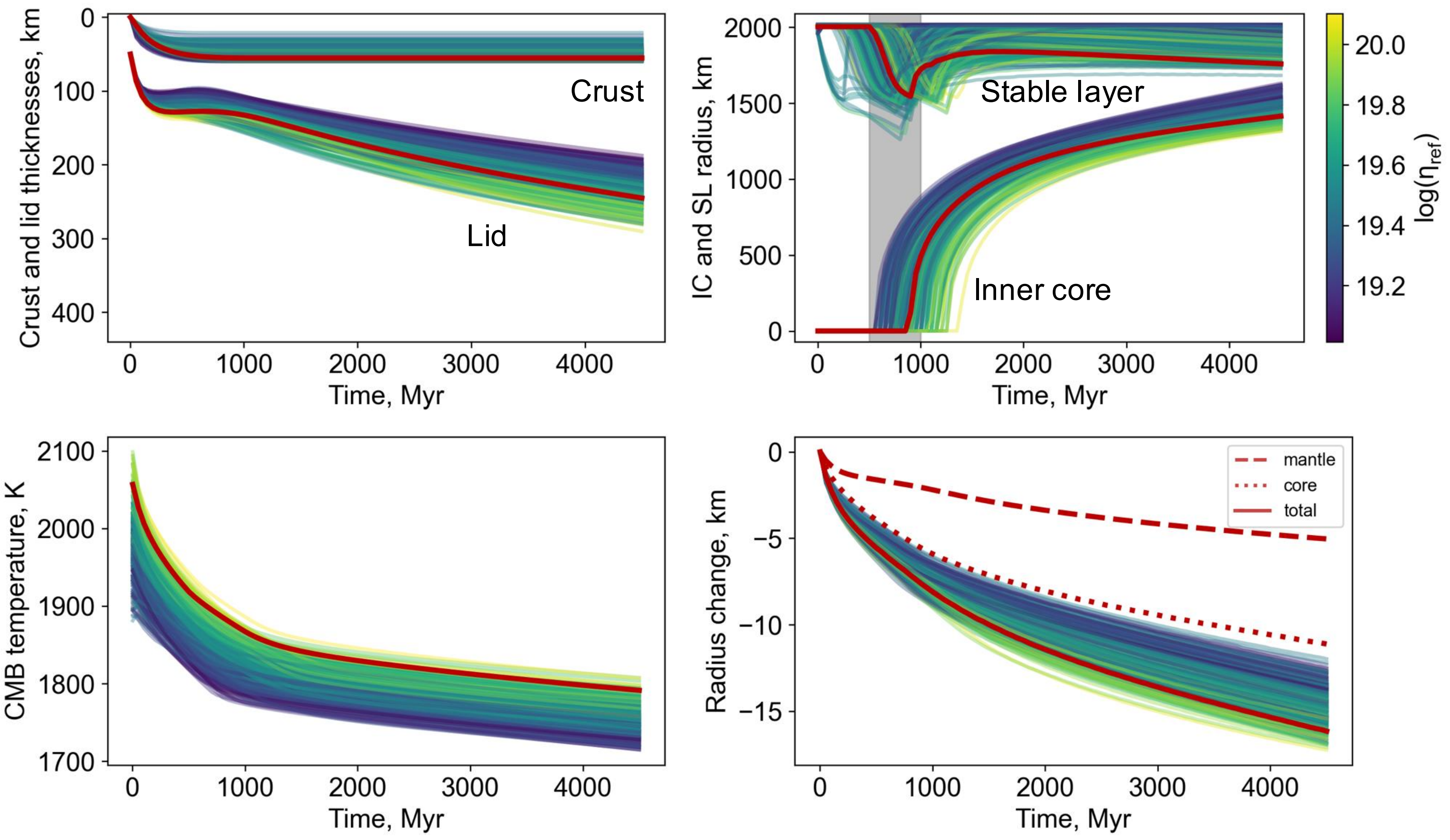

- Effective cooling in the first 1 Gyr
- Decreasing rate of radial contraction
- Inner core can crystallize after 1 Gyr
- Mantle remains partially convective

338 models (0.8%) satisfy all constraints

Crust thickness
Present-day and past dynamo
Early contraction regime
90% crust formed before 1 Gyr
50% contraction before 1 Gyr

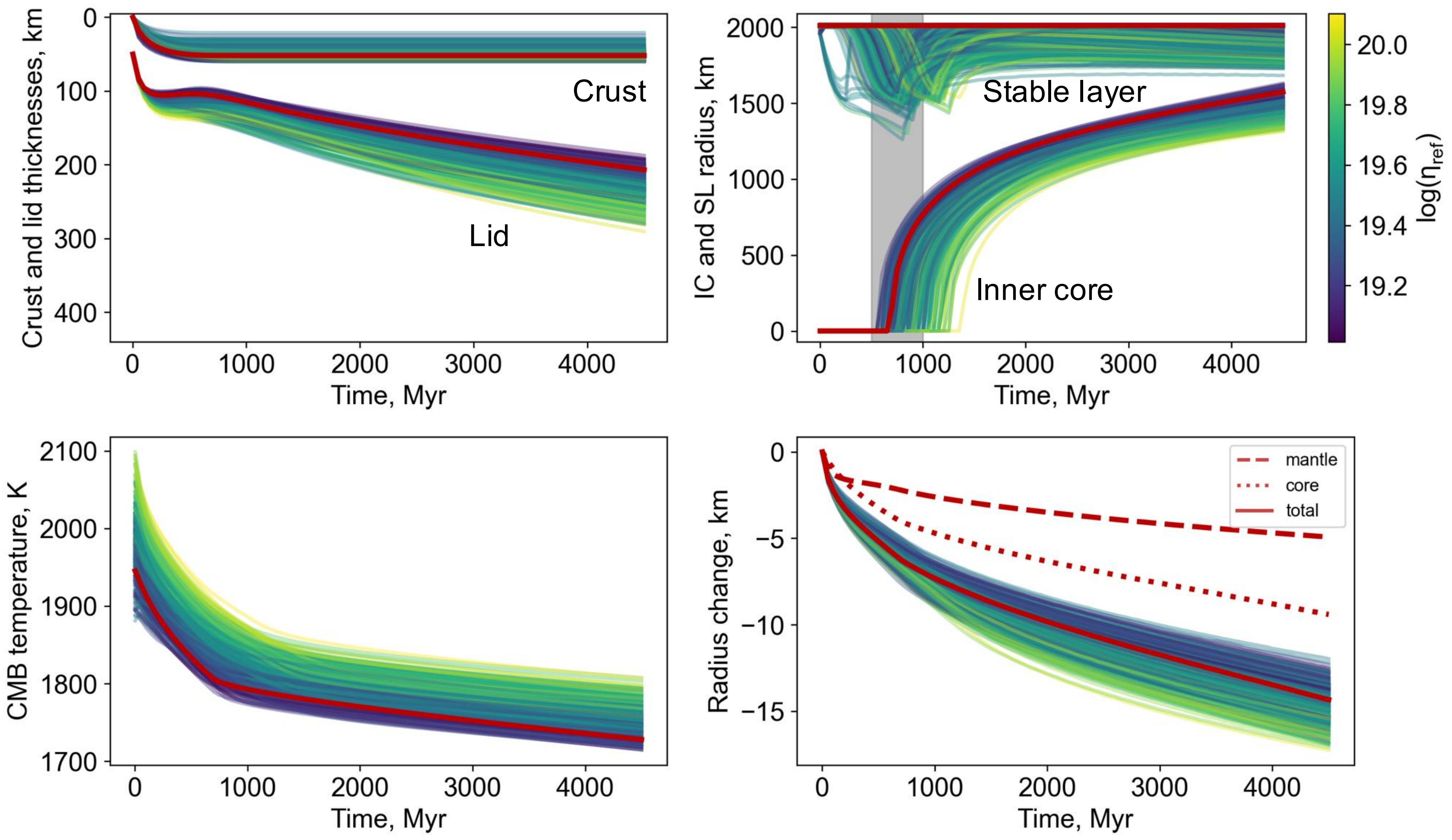

- Effective cooling in the first 1 Gyr
- Decreasing rate of radial contraction
- Inner core can crystallize after 1 Gyr
- Mantle remains partially convective
- No stable layer

338 models (0.8%) satisfy all constraints

Crust thickness
Present-day and past dynamo
Early contraction regime
90% crust formed before 1 Gyr
50% contraction before 1 Gyr

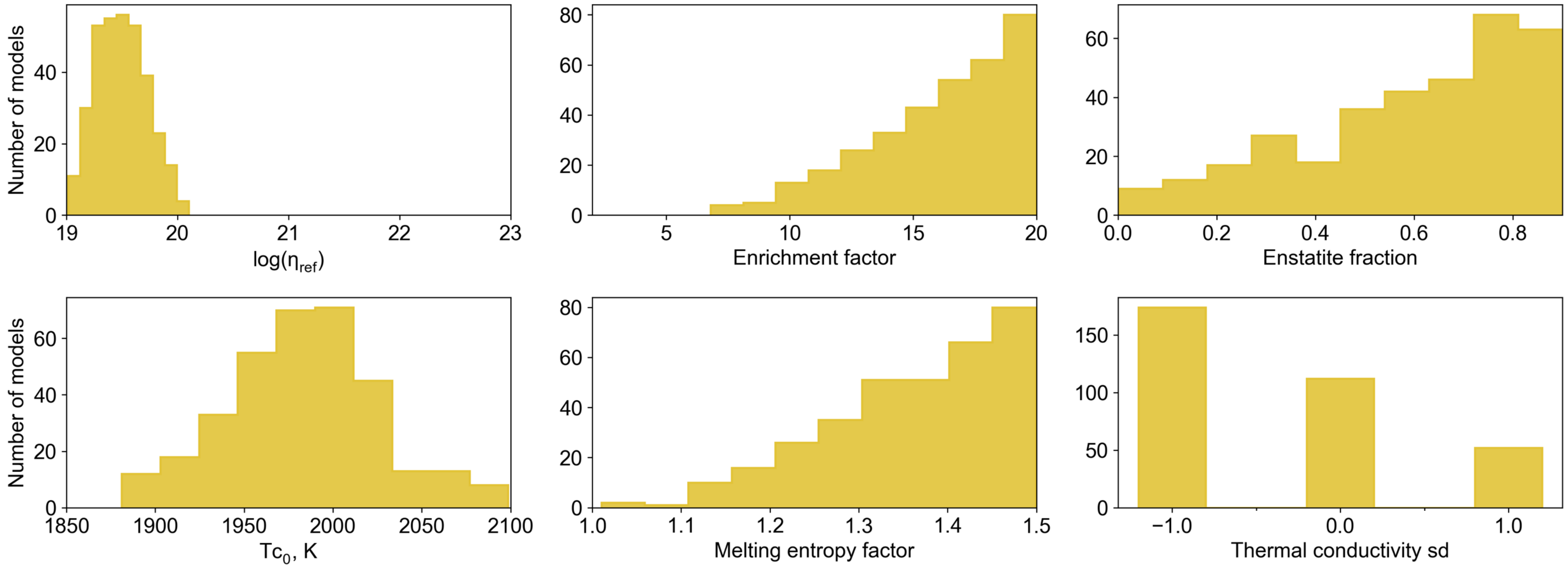

Final state of the models satisfying all constraints

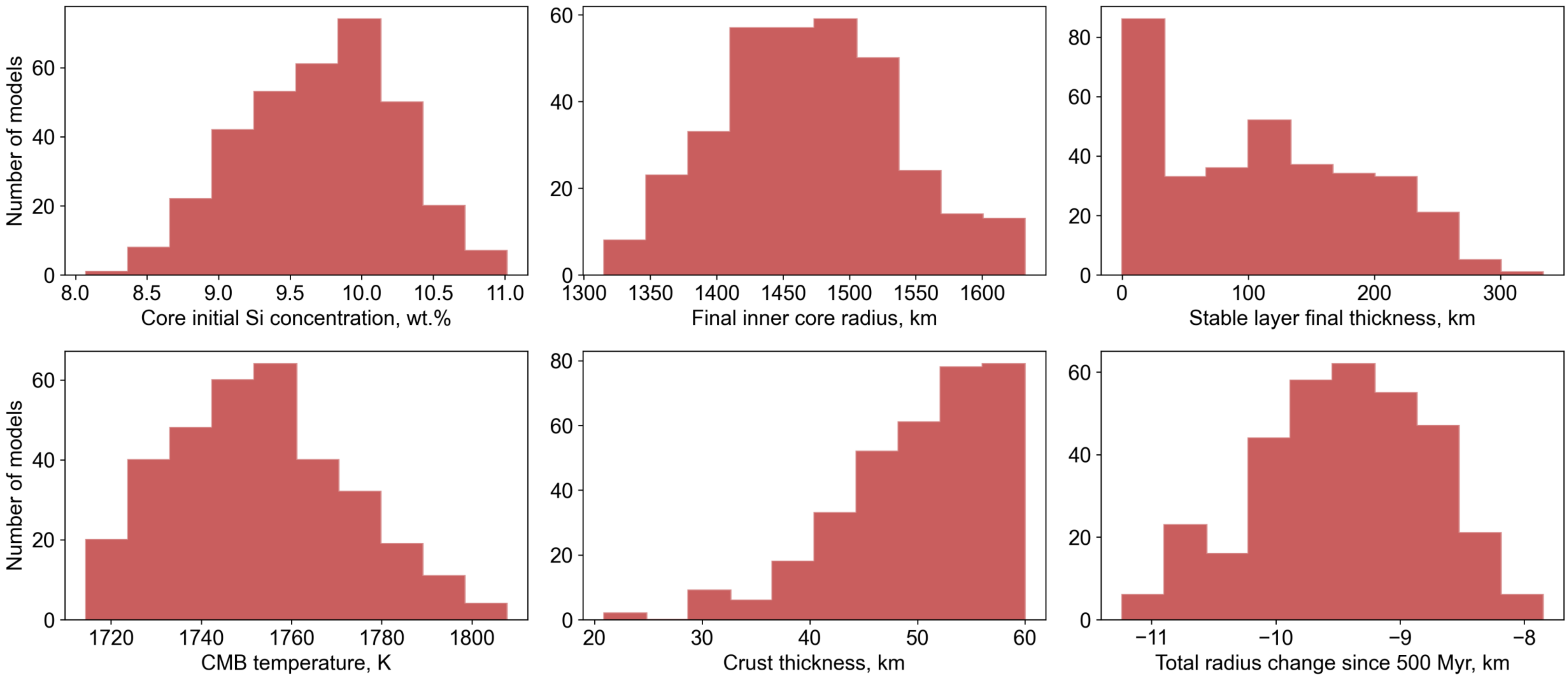

Conclusions

- We created a fully consistent thermo-chemical evolution model of Mercury

Conclusions

- We created a fully consistent thermo-chemical evolution model of Mercury
- The choice of constraints favor different “end-member” models of Mercury’s thermal evolution.

Conclusions

- We created a fully consistent thermo-chemical evolution model of Mercury
- The choice of constraints favor different “end-member” models of Mercury’s thermal evolution.

Low reference viscosity

- Ancient dynamo
- High initial contraction rates
- High initial crust production rates

High reference viscosity

- Final crust thickness
- Current dynamo action

Conclusions

- We created a fully consistent thermo-chemical evolution model of Mercury
- The choice of constraints favor different “end-member” models of Mercury’s thermal evolution.

Low reference viscosity

- Ancient dynamo
- High initial contraction rates
- High initial crust production rates

High reference viscosity

- Final crust thickness
- Current dynamo action

- Only a few intermediate models can satisfy all constraints.

Conclusions

- We created a fully consistent thermo-chemical evolution model of Mercury
- The choice of constraints favor different “end-member” models of Mercury’s thermal evolution.

Low reference viscosity

- Ancient dynamo
- High initial contraction rates
- High initial crust production rates

High reference viscosity

- Final crust thickness
- Current dynamo action

- Only a few intermediate models can satisfy all constraints.
  - Low reference viscosities, high enrichment factor and preferentially more enstatite to ensure effective cooling.

Conclusions

- We created a fully consistent thermo-chemical evolution model of Mercury
- The choice of constraints favor different “end-member” models of Mercury’s thermal evolution.

Low reference viscosity

- Ancient dynamo
- High initial contraction rates
- High initial crust production rates

High reference viscosity

- Final crust thickness
- Current dynamo action

- Only a few intermediate models can satisfy all constraints.
  - Low reference viscosities, high enrichment factor and preferentially more enstatite to ensure effective cooling.
  - Total radial contraction > 8 km, final inner core radius > 1300 km and stably stratified layer thickness < 300 km.

SI – kc and melting entropy profiles

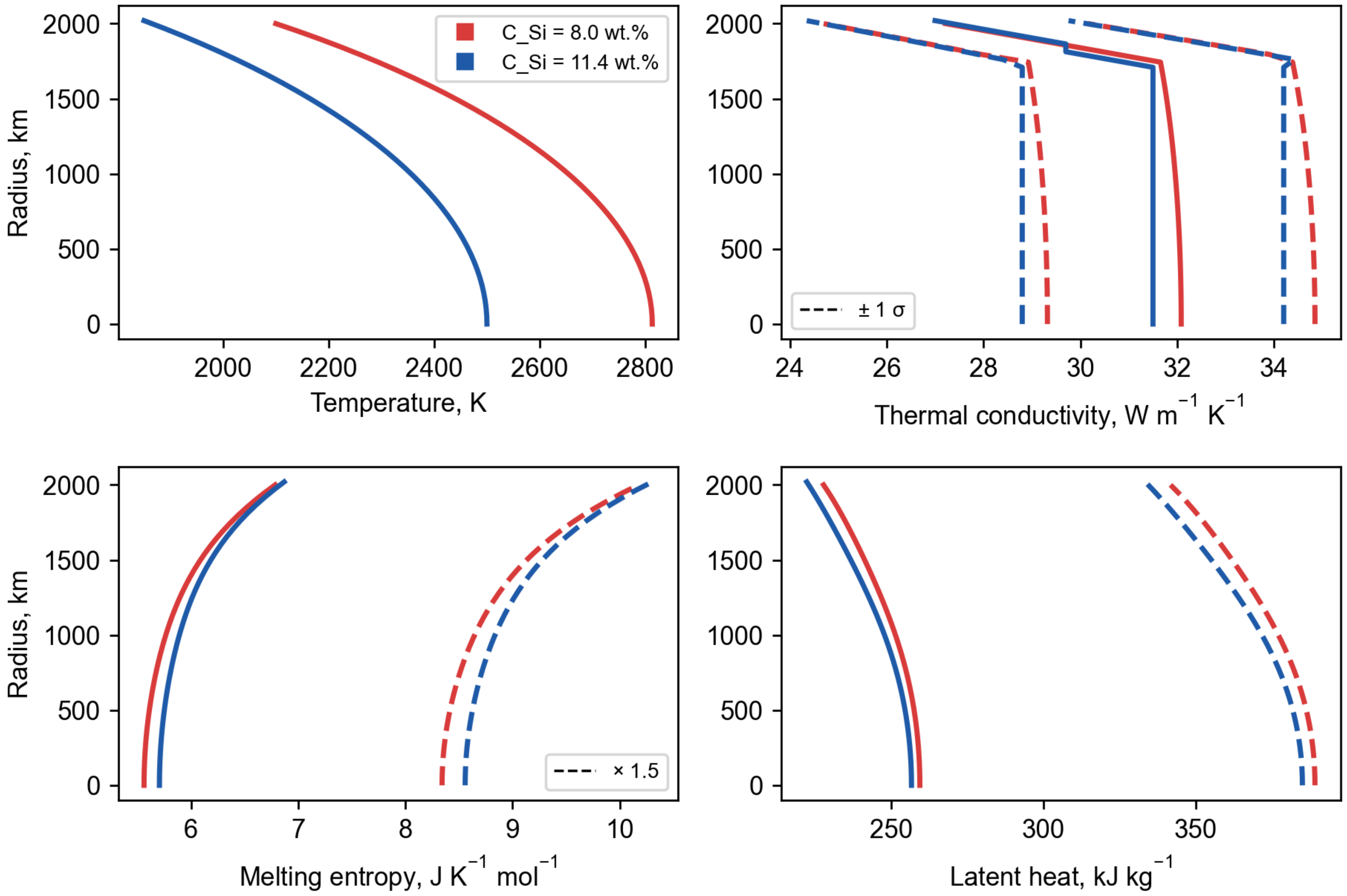

SI – profiles of core parameters

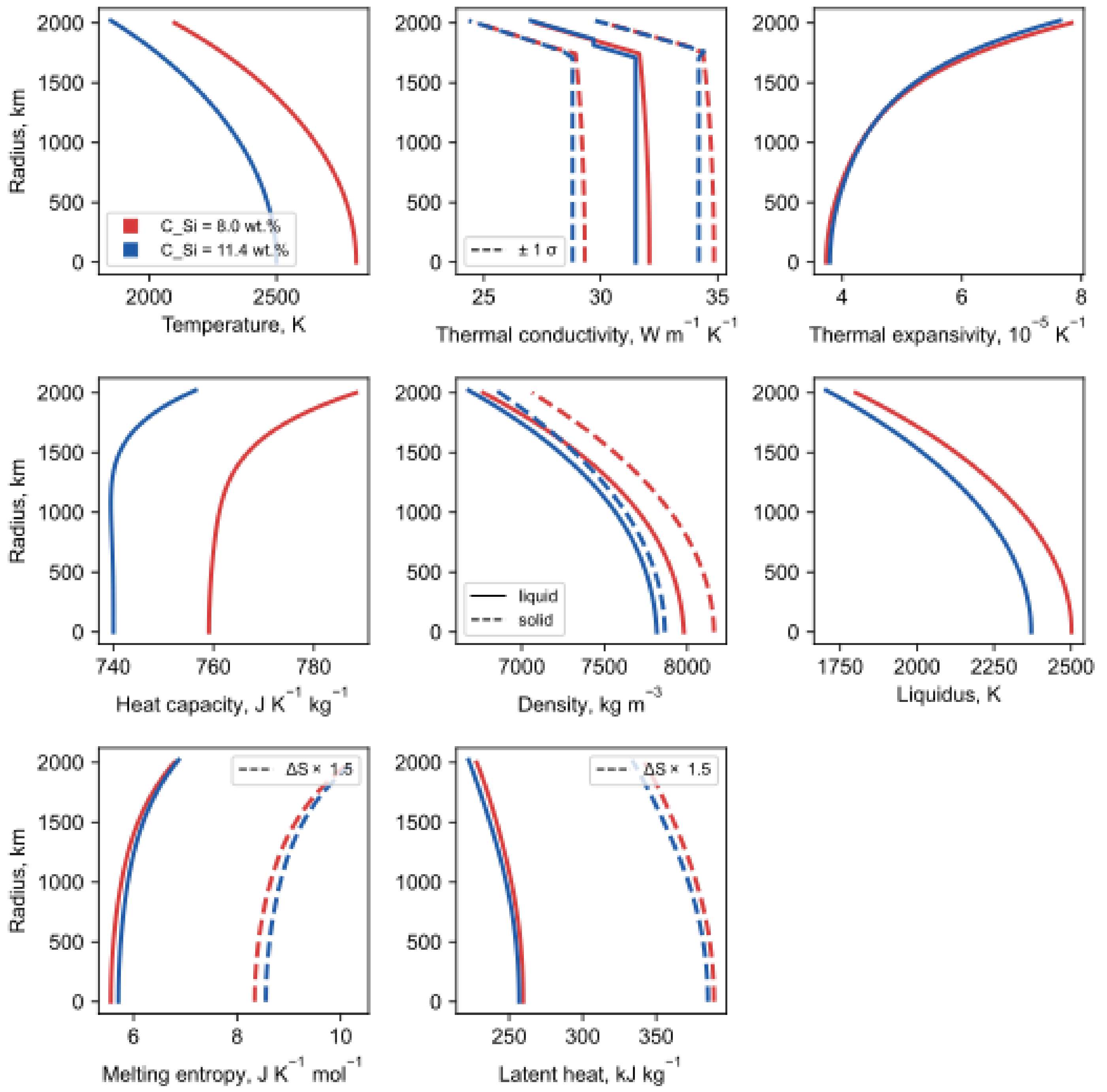

SI – profiles of mantle parameters

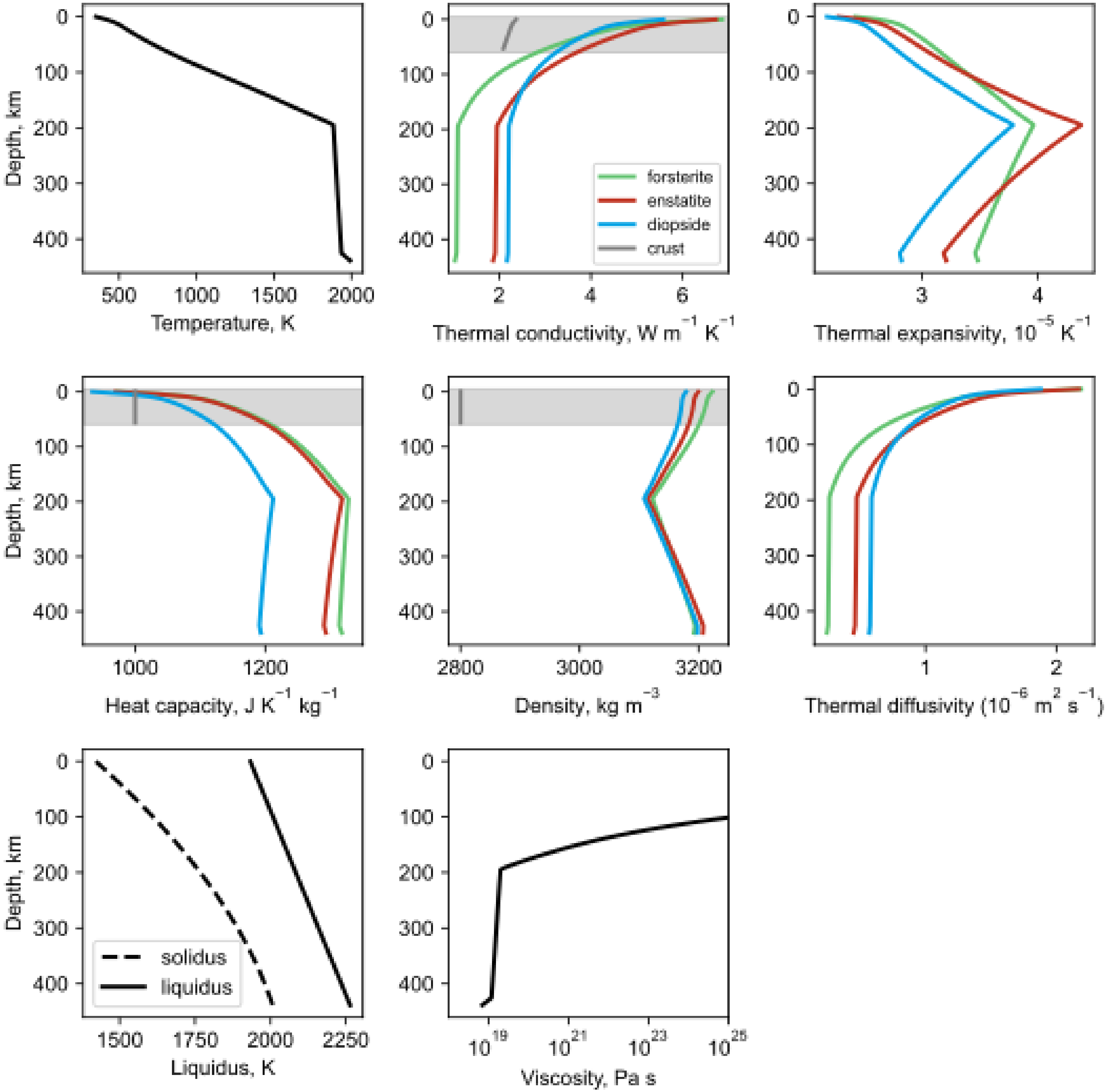

SI - Initial state of the models satisfying all constraints

Crust thickness
Present-day and past dynamo
Early contraction regime
90% crust formed before 1 Gyr
50% contraction before 1 Gyr

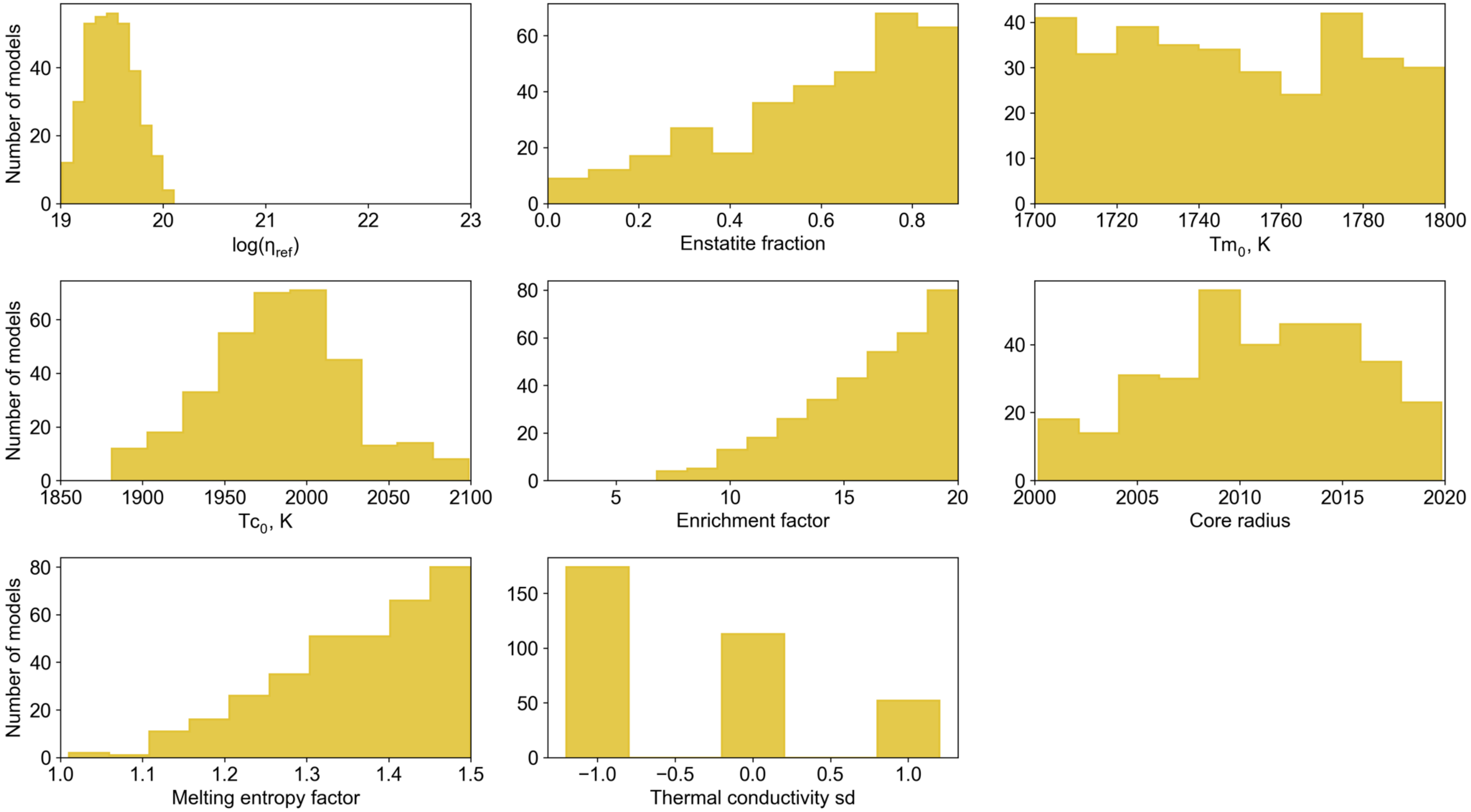

SI - Final state of the models satisfying all constraints

Crust thickness
Present-day and past dynamo
Early contraction regime
90% crust formed before 1 Gyr
50% contraction before 1 Gyr

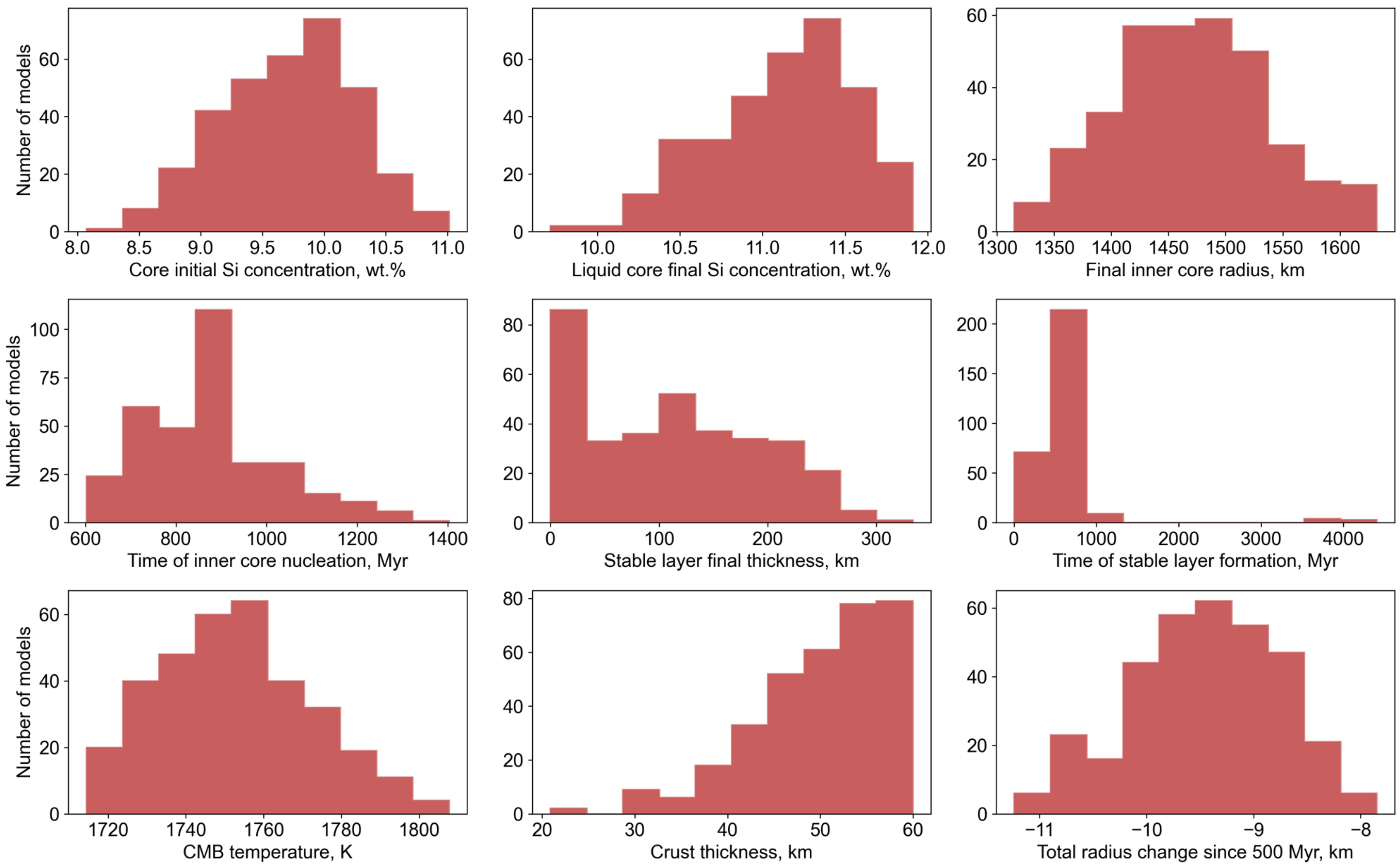

SI – Histograms for all constraints individually

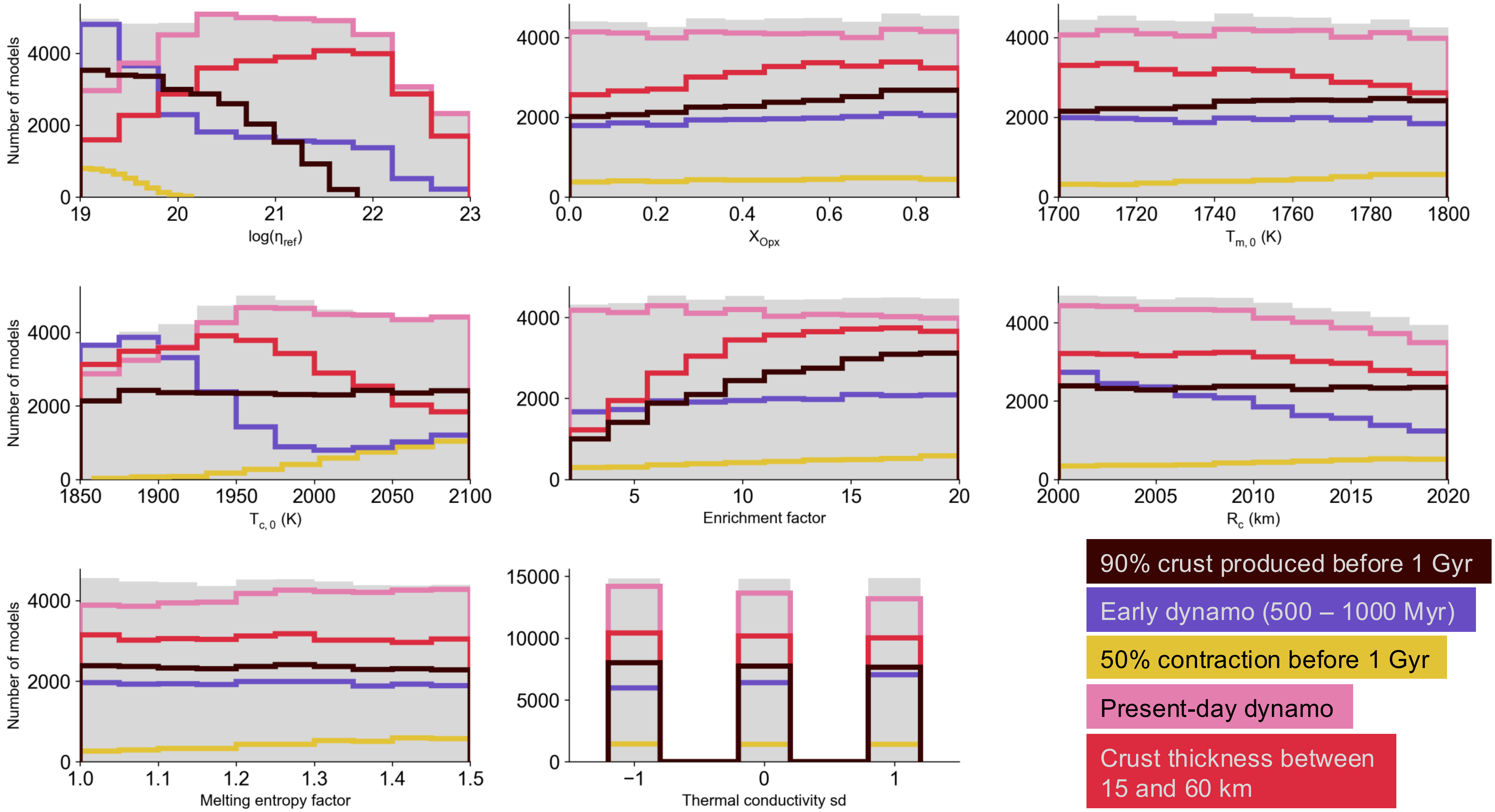

SI – Mantle model

$$T_l = T_m - a_{rh}\frac{RT_m^2}{E_a}$$

$$q_l = k_m\frac{T_m - T_l}{\delta_u}$$

$$\delta_u = (R_l - R_b) \times (\frac{Ra_{crit}}{Ra})^{\beta}$$

$$\eta = \eta_{ref} \times e^{(\frac{E_a}{RT} - \frac{E_a}{RT_{ref}})}$$

$$T_{solidus} = 1421.15 + 177 \times P - 12.2 \times P^2$$

$$T_{liquidus} = 1933.28 + 64.5 \times P - 0.048 \times P^2$$

$$k_{forsterite} = 8.114 \times (\frac{300}{T})^{1.087} \times (1 + 0.036 \times P)$$

$$k_{enstatite} = 7.667 \times (\frac{293}{T})^{0.736} \times (1 + 0.110 \times P)$$

$$k_{diopside} = (2.2516 + \frac{2020.4}{T} + \frac{47362}{T^2}) \times (\frac{1 + 0.039 \times P}{1 + 0.039 \times 13})$$

SI – Mantle model

$$
\begin{aligned}
k &= \prod_i k_i^{v_i} \\
\rho &= \sum_i v_i \times \rho_i \\
\alpha &= \sum_i v_i \times \alpha_i \\
c &= \frac{\sum_i c_i \times \rho_i \times v_i}{\rho}
\end{aligned}
$$

$$T(z) = T_0 \times exp(\frac{\alpha_0 \times g \times (z - z_0)}{c_0})$$

SI – Mantle model

Parameter	Value
Time-step, dt	2.5 Myr
Initial lid thickness, D_{lid_0}	50 km
Planet radius, R_p	2440 km
Surface temperature, T_s	350 K (Tosi et al., 2025)
Initial TBL thickness	10 km
Gravitational acceleration, g	3.7 m s^{-2}
Crust density, ρ_{cr}	2800 kg m^{-3}
Critical Rayleigh number, Ra_{crit}	450
Upper TBL thickness exponent, β^u	0.335 (Thiriet et al., 2019)
Lid temperature factor, a_{rh}	2.54 (Thiriet et al., 2019)
Convective velocity scale, u_0	2×10^{-12} m s^{-1}
Viscosity reference temperature, T_{ref}	1600 K
Creep activation energy, E_a	300 kJ mol^{-1}
Mantle latent heat of melting, $\mathcal{L}$	6×10^5 J kg^{-1}
Specific heat capacity of the crust, C_{cr}	1000 J kg^{-1} K^{-1}
Uranium concentration	35 ppb (Pirotte et al., 2023)
Thorium concentration	121 ppb (Pirotte et al., 2023)
Potassium concentration	356 ppm (Pirotte et al., 2023)

SI – Core model

$$q_c = k(T_c, P_c)\frac{T_c - T_b}{\delta_c}$$

$$\delta_c = (\frac{\kappa_b \eta_c Ra_{i,cr}}{\alpha_b \rho_m g(T_c - T_b)})^\beta$$

$$Ra_{i,cr} = 0.28 Ra_{int}^{0.21}$$

$$Ra_{int} = \frac{\rho_m g \alpha_m (T_m - T_s + T_c - T_b)(R_p - R_c)^3}{\kappa_m \eta_m}$$

$$Q_c = Q_s + Q_g + Q_l$$

$$E_J = E_s + E_s + E_g - E_k$$

$$T_{liq}^i = T_0^i \times [\frac{P}{a^i} + 1]^{\frac{1}{c^i}}$$

	T_0	a	c
Fe	1810.91	15.4789	2.84968
Eutectic	1538	24.66	2.17

SI – Core model

$$T_{liq}^{i} = T_{0}^{i} \times [\frac{P}{a^{i}} + 1]^{\frac{1}{c^{i}}}$$

	T_0	a	c
Fe	1810.91	15.4789	2.84968
Eutectic	1538	24.66	2.17

$$T_{liq} = T_{liq}^{Fe} - (T_{liq}^{Fe} - T_{liq}^{E}) \times \frac{x_{Si}}{x_{Si}^{E}}$$